Jour. Fac. Sci., Hokkaido Univ., Ser. VII (Geophysics), Vol. 11, No. 1, 363-381, 1998.

Hydrometeor Size Distribution Estimated by Vertically Pointing Doppler Radar and Polarimetric Radar Measurements —— Preliminary Results ——

Masayuki Maki

Atmospheric and Hydrospheric Science Division, National Research Institute for Earth Science and Disaster Prevention, Tsukuba 305-0006, Japan

Koyuru Iwanami

Nagaoka Institute of Snow and Ice Studies, National Research Institute for Earth Science and Disaster Prevention, Nagaoka 940-0821, Japan

Masao Higashiura*, Takeshi Sato

Shinjo Branch of Snow and Ice Studies, National Research Institute for Earth Science and Disaster Prevention, Shinjo 996-0091, Japan

Hiroshi Uyeda,

Division of Earth and Planetary Sciences, Graduate School of Science, Hokkaido University, Sapporo 060-0810, Japan

Hiroshi Hanado and Hiroshi Kumagai

Kashima Space Research Center, Communication Research Laboratory, Kashima 314-0012, Japan

(Received December 15, 1997)

Abstract

Hydrometeor size distribution (HSD) was estimated by two independent methods ; One was a vertically pointing Doppler radar (VPR) method and the other a polarimetric radar (POL) method. In situ measurements of raindrop size distribution by a Joss-Waldvogel type disdrometer were also carried out to acquire ground truth data.

* Present affiliation: Nagaoka Institute of Snow and Ice Studies, National Research Institute for Earth Science and Disaster Prevention, Nagaoka 940-0821, Japan.

The median volume diameter D_0 of the exponential HSD estimated by the VPR method agreed well with disdrometer measurements. According to error analysis, D_0 can be estimated within an error of 30% (in the case of rain) and 60% (in the case of snow) if the average terminal velocity of the precipitation particles in the radar sampling volume is estimated within an error of 20%. On the other hand, the estimation error for N_0 by the VPR method is 200% (rain) and 460% (snow) for the same estimation error of the average terminal velocity. D_0 estimated by the POL method is qualitatively in agreement with the disdrometer measurements. Although there are difficulties in correcting the attenuation effect of precipitation on polarimetric parameters, it is demonstrated that X-band polarimetric radar can be used to study precipitation processes.

1. Introduction

Although the estimation of precipitation parameters such as hydrometeor size distribution (hereafter noted as HSD), liquid water content, and precipitation intensity is a classical theme, it is still one of the major and unsolved problems in cloud physics and radar meteorology. Information on the spatial distribution of precipitation parameters and their time evolution are required in order to improve our understanding of the precipitation mechanism. An other motivation for the present study was to establish algorithm that provides ground truth data for the Tropical Rainfall Measurement Mission (TRMM). Not only horizontal distribution of rainfall amount but also vertical profiles of precipitation parameters are necessary for understanding the mechanism of tropical precipitation systems and for the quantitative analysis of heat and water budgets in tropical areas.

Weather radar is a useful tool in obtaining precipitation parameters. Vertically pointing Doppler radar has been used to estimate HSD by many researchers (Rogers and Pilie, 1962 ; Caton, 1966 ; Sekhon and Srivastava, 1971 ; Atlas *et al.*, 1973 ; Hauser and Amayenc, 1981). It was shown by Seliga and Bringi (1976) that well-calibrated polarimetric radar can be used to estimate exponential raindrop size distribution. The present study will focus on methodology of radar meteorology, its purposes being 1) to develop an algorithm for the estimation of precipitation parameters utilizing vertical pointing Doppler radar and polarimetric radar, and 2) to compare these estimation results and to analyze the accuracy of each estimation method. Although detailed studies on the precipitation mechanism are beyond our purposes, some of the microphysical processes of the observed prefrontal rain band were discussed in view of the estimation results.

2. Measurements

Observations were made in November 1994 on the Ishikari Plain, Hokkaido, Japan. Two X-band radar systems of the National Research Institute for Earth Science and Disaster Prevention (NIED) were used. One of the systems has polarimetric capability and the other is a Doppler radar operating with vertical pointing mode. Radar operation is shown schematically in Fig. 1. RHI and PPI reflectivity factor data, and two polarimetric parameters (Z_{DR}, *LDR*) were measured every 5 minutes by radar 1. Vertical profiles of reflectivity factor and Doppler velocity were measured every 20 seconds by radar 2. Its range resolution was 62.5 m. The distance between the two radar systems was 20.7 km. The raindrop size distribution was also measured at the height of 2.4 m by a Joss-Waldvogel type disdrometer at the site of radar 2. This was used for radar calibration and for ground truth data of the radar-derived raindrop size distribution.

Observations with the NIED linear polarimetric radar (radar 1) were the first following its completion in 1994. Measurements in various combinations of polarization pattern were carried out during test operations. We could derive the distributions of differential reflectivity Z_{DR} while it was unfortunately

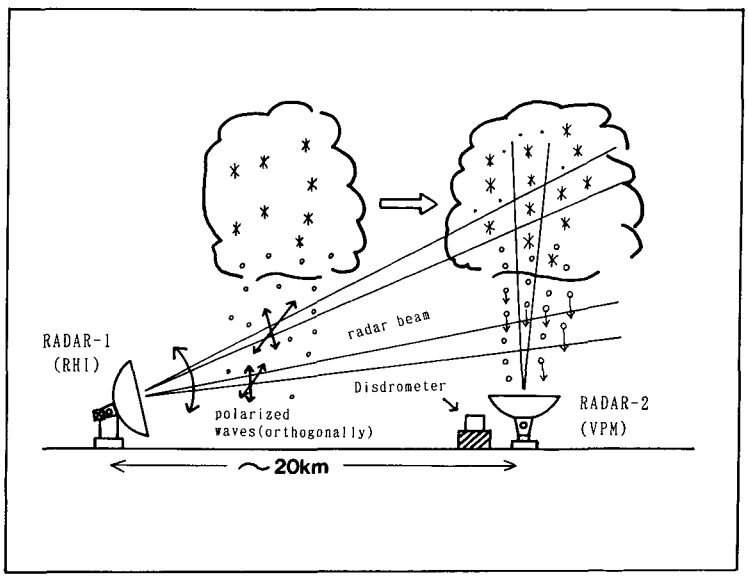

Fig. 1. Schematic picture showing measurements of precipitation by polarimetric radar, vertically Doppler Doppler pointing radar and disdrometer.

Table 1. Specifications of the NIED Dual-Polarization Doppler Radar.

Antenna Reflector	2.2 m Aperture, Circular Parabola
Beam-width	$\leqq$1.25° in Horizontal and Vertical
Antenna Gain	$\geqq$42 dB
Polarization	Horizontal or Vertical (Transmitted & Received)
Antenna Scan Coverage	0~360° Azimuth −2~182° Elevatoin
Antenna Scan Rate	0.5/1/2/3/6 rpm, Horizontal 1/2/3 rpm, Vertical
Transmitting Frequency	9,445 MHz
Transmitting Peak Power	40 kW
Pulse-width	0.5 μs, Doppler Mode 1.0 μs, Dual-Polarization Mode
Pulse Repetition Frequency	2,000 Hz/1,500 Hz, Doppler Mode 1,000 Hz, Dual-Polarization Mode
Min. Detectable Signal	$\leqq -110$ dBm
Max. Range	64 km
Range Resolution	62.5/125/250 m
Velocity Range	$\pm$15.88 m/s ($\pm$47.6 m/s, Stagger PRF)
Velocity Resolution	12.4 cm/s (37.2 cm/s, Stagger PRF)
Data Recording Media	8 mm Cartridge Magnetic Tape

difficult to estimate cross-polarization signals precisely because of the isolation problem of the polarization switch. Main specifications for the NIED polarimetric radar are listed in Table 1. Specification for radar 2 are presented in Maki *et al.* (1989).

3. Methods

3.1 Vertically Pointing Doppler Radar (VPR) method

A thorough review of techniques for deducing HSD from measurements by vertically pointing Doppler radar system is presented by Atlas *et al.* (1973). The method used in the present study is similar to Rogers (1964) and is based on the following assumptions. Hereafter, this method is referred to as VPR method.

(1) HSD is represented by the exponential distribution function,

$$N(D)=N_0\exp[-G(D/D_0)], \tag{1}$$

where, $N(D)$ is the number of hydrometeors of diameter D per unit volume, N_0

the interception parameter of the exponential HSD, D_0 the median-volume diameter defined as the drop size above which half the liquid water is found. The parameter $G=3.67$ if the exponential function (1) of HSD is defined from $D=0$ to $D=\infty$. In practice, $G\approx 3.67$ if the maximum diameter $D_{\max}\geqq 2.5\ D_0$ and the minimum diameter $D_{\min}=0$ or if $D_{\min}\leqq 0.3\ D_0$ and $D_{\max}=\infty$ (Atlas *et al.*, 1973).

(2) Terminal hydrometeor fall speed w_t is represented by

$$w_t=aD^b(\rho_0/\rho)^{0.4}, \tag{2}$$

where, $(\rho_0/\rho)^{0.4}$ is the correction factor, which accounts for the change in air density with height (Foote and du Toit, 1969). ρ is the air density at the level of observation and ρ_0 is the air density at ground level. The parameters a and b are constants dependent on the type of precipitation particles. In this paper, $a=386.6$, $b=0.67$ for raindrops (Atlas and Ulbrich, 1977) and $a=8.34$, $b=0.31$ for snowflakes (Gunn and Marshall, 1958) are used.

(3) The hydrometeor size is much smaller than the radar wavelength so that Rayleigh approximation concerning back scattering in precipitation can be assumed. Thus, the equivalent radar reflectivity factor Z_e is defined by

$$Z_e=\int_0^\infty N(D)D^6dD. \tag{3}$$

(4) Average terminal hydrometeor velocity $\overline{W}_t$ in the radar sampling volume is related to equivalent radar reflectivity factor Z_e by the following function.

$$\overline{W}_t=pZ_e^q(\rho_0/\rho)^{0.4}, \tag{4}$$

where, parameters p and q are constants which may depend on the type of precipitation. According to the experimental findings by Joss and Waldvogel (1970), $p=-2.6$ and $q=1/9.3$ for rainfall. Joss and Waldvogel (1970) obtained these values from actual drop size data at the ground in seven different storms and showed its accuracy was ± 1 m/s for $10<Z_e<2\times 10^5$ mm^{6}mm^{-3}. Rogers (1964) proposed $p=3.8$, $q=0.071$. For snowflakes, Atlas *et al.* (1973) used $p=0.817$, $q=0.063$ based from Gunn and Marshall (1958) size spectrum of snow particles.

In addition to the above assumptions, we use the definition of $\overline{W}_t$ to derive a set of equations to estimate HSD and vertical air speed. $\overline{W}_t$ is defined by

$$\overline{W}_t=\frac{\int_0^\infty w_t(D)N(D)D^6dD}{\int_0^\infty N(D)D^6dD}. \tag{5}$$

If we use equations (1) and (2), we obtain

$$\overline{W}_t=a\left(\frac{D_0}{G}\right)^b\frac{\Gamma(7+b)}{\Gamma(7)}\left(\frac{\rho_0}{\rho}\right)^{0.4}, \tag{6}$$

where, Γ is the gamma function defined by

$$\Gamma(n+1)=\int_0^\infty x^n\exp(-x)dx=n!. \tag{7}$$

From equations (1) and (3), we obtain

$$Z_e=N_0D_0^7\frac{\Gamma(7)}{G^7}. \tag{8}$$

Equations (4), (6), and (8) are used to calculate HSD parameters (N_0 and D_0). Once Z_e is measured by vertically pointing Doppler radar, $\overline{W}_t$ is calculated by (4), then, D_0 is calculated by (6) and N_0 is calculated by (8). Measured Z_e usually contains some error due to the fact that Rayleigh assumption is not always satisfied and the calibration of radar systems is not perfect. In this paper, we calibrated radar measured Z_e by using the disdrometer derived Z_e. The vertical air speed $\overline{W}_a$ is calculated by

$$\overline{W}_a=\overline{V}_D-\overline{W}_t, \tag{9}$$

where, $\overline{V}_D$ is the measured average Doppler velocity.

Once the HSD is estimated by the procedures mentioned above, the other precipitation parameters such as liquid water content, total number of particles, and precipitation rate can be calculated (Maki *et al.*, 1998).

3.2 Polarimetric Radar (POL) method

Seliga and Bringi (1976) proposed a technique to estimate HSD parameters (D_o and N_0) by using polarimetric radar measurements. Hereafter this method is refered to as POL method. Horizontal and vertical radar reflectivity, $Z_{H,V}$ for the truncated HSD is represented by

$$Z_{H,V}=\frac{\lambda^4}{\pi^5|K|^2}\int_0^{D\max}\sigma_{H,V}(D)N(D)dD, \tag{10}$$

where,

$$|K|^2=\left|\frac{m^2-1}{m^2+1}\right|^2, \tag{11}$$

λ: radar wavelength,

m: complex refractive index of water,

$\sigma_{H,V}(D)$: radar cross section.

Normalized horizontal reflectivity factor, Z_H/N_0, is defined as

$$\frac{Z_H}{N_0}=\frac{\lambda^4}{\pi^5|K|^2}\int_0^{D\max}\sigma_H(D)\exp[-G(D/D_0)]dD. \tag{12}$$

Differential reflectivity, Z_{DR} is defined as the ratio between Z_H and Z_V:

$$Z_{DR}=10\log\left(\frac{Z_H}{Z_V}\right)=10\log\left[\frac{\int_0^{D\max}\sigma_H(D)\exp[-G(D/D_0)]}{\int_0^{D\max}\sigma_V(D)\exp[-G(D/D_0\}]}\right]. \tag{13}$$

where, $D_{\max}$ is the maximum diameter of a raindrop. The relationships of differential reflectivity Z_{DR} and normalized horizontal reflectivity $10\log(Z_h/N_0)$ to

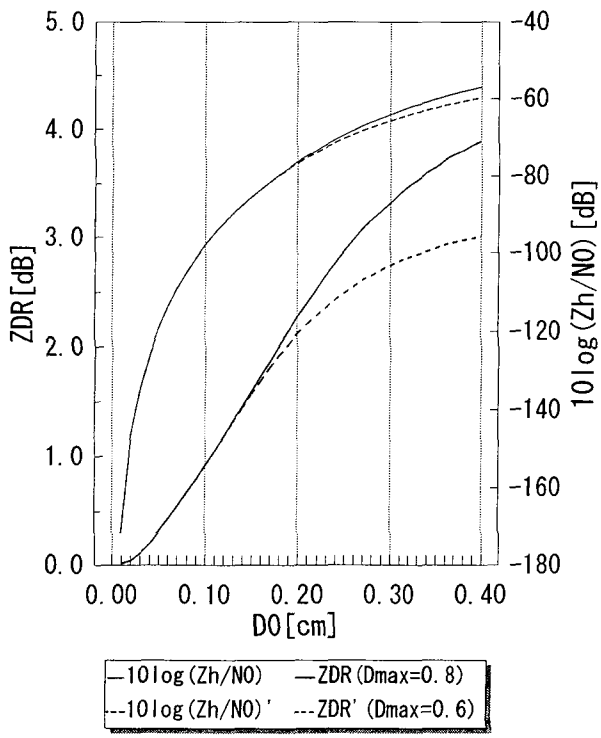

Fig. 2. Differential reflectivity Z_{DR} and normalized horizontal reflectivity $10\log(Z_h/N_0)$ as a function of median volume drop diameter D_0.

median volume drop diameter D_0 were calculated by the method of Seliga and Bringi (1976) and Seliga *et al.* (1981) and are shown in Fig. 2. Calculations were made for a radar wavelength of 3.18 cm and refractive index of water at 10°C. Values of D_0 and N_0 were estimated from observed Z_{DR} and Z_h by using the relationships shown in Fig. 2.

4. Results

4.1 Precipitation bands on November 6 and 11, 1994

During the observation period, two rainfall events were observed. The first one was observed on November 6, 1994, the other on November 11, 1994. Although both events were associated with the passage of low depressions and developed in the warm sector of frontal systems. The former event was more stratiform rain type compared to the latter case. According to the vertical profiles of average Doppler velocity and average reflectivity factor during the passage of the rain band on November 6, the melting layer was clearly recognized as being from a height of 2.1 km to 2.6 km, which is one of the signatures of stratiform precipitation. Below this level, a rapid increase in Doppler velocity was seen, which might be due to the melting of snowflakes. In the latter case, an updraft existed above the bright band during the majority of the period when the rain band was passing over the radar site. The following sections will focus on the case of November 6.

4.2 HSD estimated by vertically pointing Doppler radar (VPR) method.

The time sequence of GMS images and PPI images of Sapporo city radar showed clearly a precipitation system passing over the site of radar system 1 from 17 : 30 to 22 : 30 JST. A radio sounding at Sapporo, which was made just before the passage of the rain band, showed the thermal stratification was convectively unstable at a height from 0.1 km to 2.5 km.

Time height cross sections of reflectivity factor and Doppler velocity obtained by vertically pointing Doppler radar are shown in Fig. 3. Four precipitation echoes were observed ; C1 (18 : 00 JST), C2 (18 : 30 JST), C3 (18 : 45–20 : 15 JST) and C4 (20 : 30–22 : 15 JST). Figure 4 shows the locations of these echoes schematically. The echoes moved 36° in a counterclockwise direction from the north with a speed of 54 km/h (=15 m/s). The rain band orientation was very close to but smaller than its propagation direction. It should be noted that the evolution of the rain band during the observation period from 17 : 30 JST to 22 : 30 JST is not considered in Fig. 4 because the aim of the figure is to show only

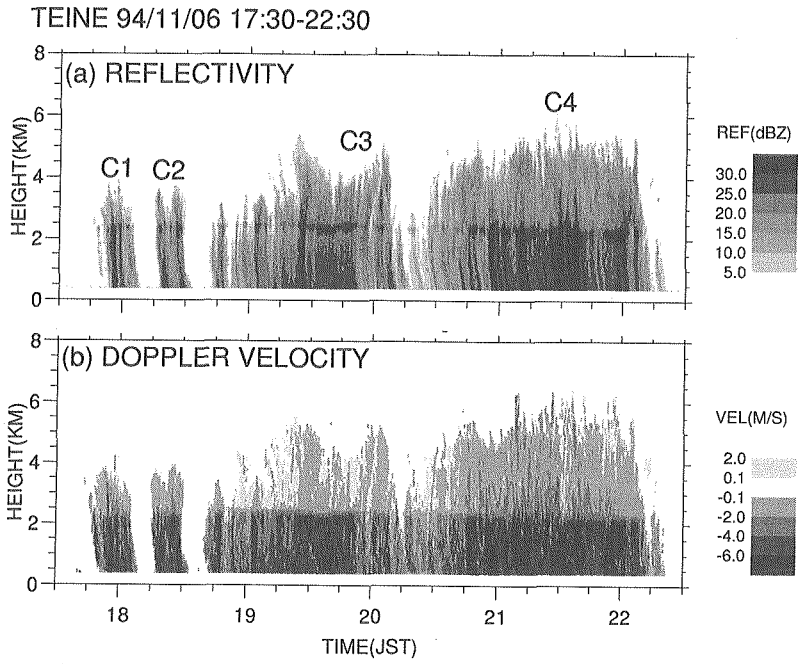

Fig. 3. Time-height cross section of reflectivity factor (a) and Doppler velocity (b) of the warm-sector rain band observed on November 6, 1994.

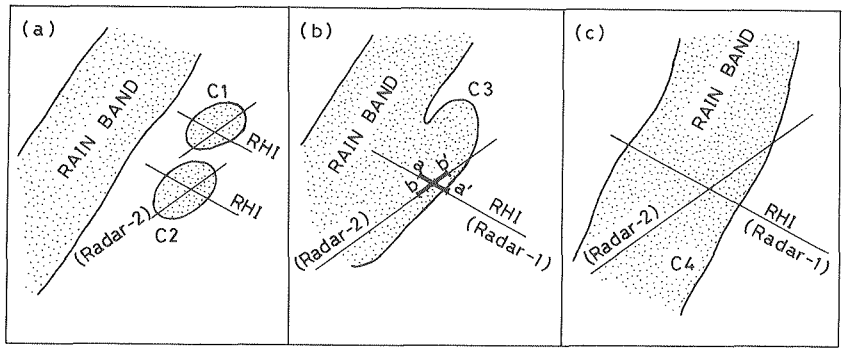

Fig. 4. Schematic PPI images of the observed precipitation echoes showing the locations of C1, C2, C3 and C4 relative to radar 2. Azimuth angles of RHI scan of radar 1 are also shown. In the figure, evolution of each echo was not considered.

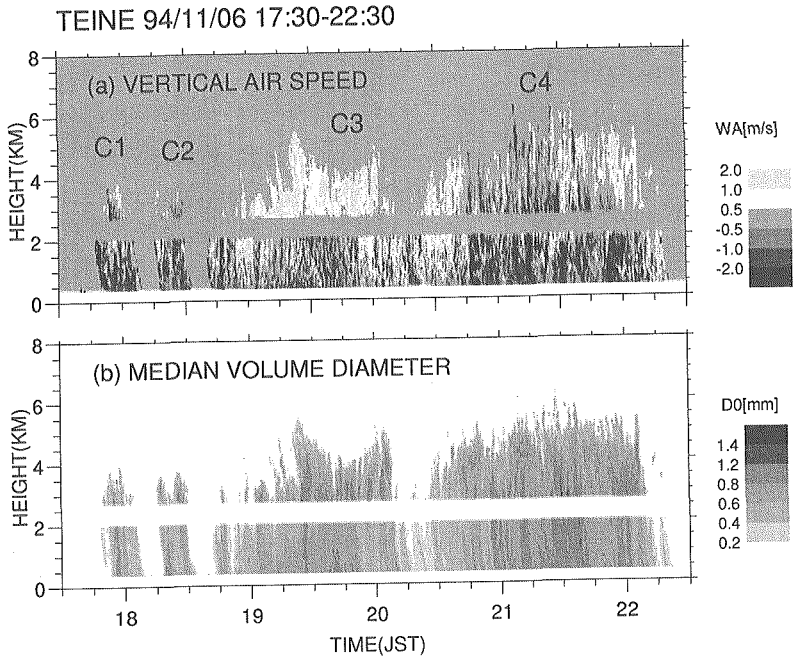

Fig. 5. Time-height cross section of vertical air velocity (a) and D_0 estimated by vertically pointing Doppler radar observation.

the relative location of each precipitation cell. The echo cells C1 and C2 were small isolated precipitation echoes, which had a diameter of less than 10 km. These isolated echoes might be related with a maijor rain band dynamically. The C3 echo cell was located on the southeast side of the major rain band. The C4 echo was located in the major rain band.

Time-height cross sections of estimated vertical air velocities $\overline{W}_a$ and median volume diameter D_0 are shown in Fig. 5. It is difficult to estimate HSD in the melting layer because the interpretation of radar reflectivity factor from the melting layer is complicated. Ice particles covered with water in this layer act as large water drops for back scattering and thus Rayleigh assumption is not satisfied. Although additional information on hydrometeor type, and factors such as surface condition are necessary to estimate HSD above the melting layer, we assume that hydrometeor above the melting layer is snow.

An updraft larger than 1 m/s existed in the C3 precipitation cell from 18 : 45 to 20 : 15 JST. On the other hand, a down draft of about 1 m/s began from the height of 4 km, which was just above the melting layer from 21 : 00 to 22 : 00

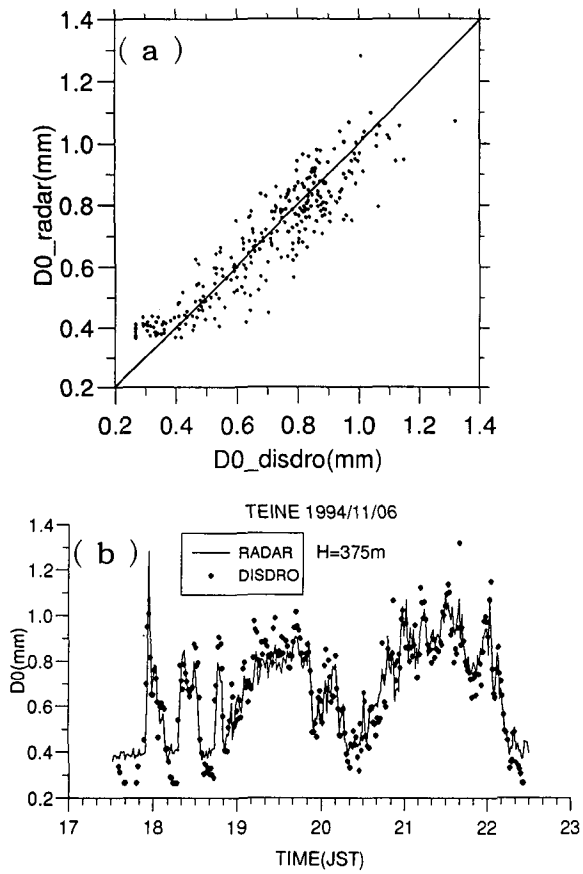

Fig. 6. Comparison of radar estimated D_0 with D_0 measured by disdrometer.

JST. At the center of precipitation cells C3 and C4, D_0 increased with lowering height. Comparison between radar estimated D_0 and disdrometer measured D_0 (Fig. 6) showed good agreement with each other, with the exception of small values of D_0 to which radar is not sensitive.

4.3 HSD estimated by polarimetric radar (POL) method

RHI images of horizontal reflectivity Z_h and differential reflectivity Z_{DR} for the C4 echo are shown in Fig. 7. The maximum positive values for Z_{DR} were observed at a height near the bright band where the maximum values of horizontal reflectivity Z_h were also observed.

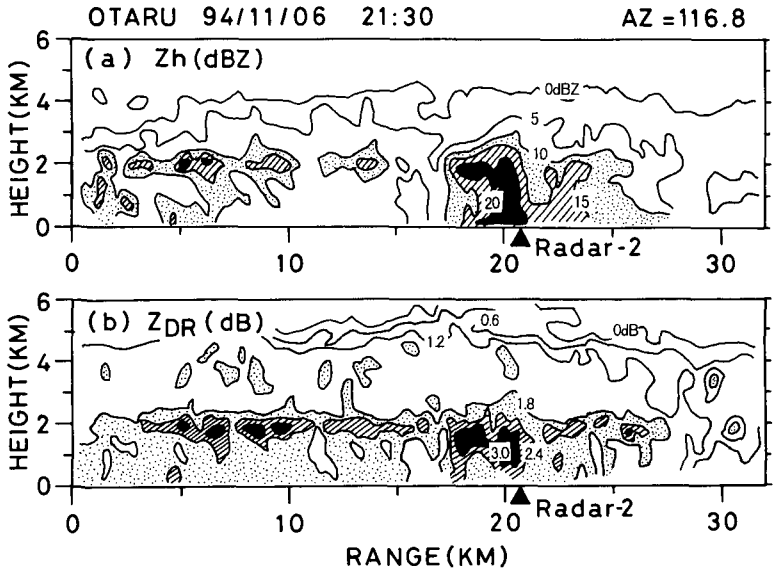

Fig. 7. RHI images of azimuth of 116.8 degrees at 21 : 30 JST on November 6, 1994. Top and bottom images represent horizontal reflectivity and differential reflectivity, respectively. The black triangle symbol on the axis of abscissas shows the location of radar 2.

The black triangle on the axis of abscissas shows the location of radar 2. While the location of radar 2 was not at the center of echo C3, it was very close to the region with maximum reflectivity factor for echo C4.

Figure 8 indicates the time series for median volume diameter D_0 derived from disdrometer and polarimetric radar from 19 : 00 to 20 : 00 JST on November 6. D_{0dis} denotes D_0 estimated from disdrometer measurements and D_{0zdr} estimates that from Z_{DR} using the method described in section 3.2. Z_{DR} values in the mesh of 500 m horizontal × 250 m vertical at the height of 625 m on RHI above the radar-2 site were used for the estimation, and values of D_{0dis} were averaged over two minutes in consideration of the falling time of raindrops. Rainfall rates over one minute ranged from 0.15 to 2.80 mm/h for this period.

The tendency of time variations for both D_{0dis} and D_{0zdr} shows very good agreement, although D_{0zdr} values are about twice as much as D_{0dis}. Effects related to attenuation may be one of the reasons for the discrepancy. Assuming that D_{0dis} values were true, the following relationship between D_{0dis} and D_{0zdr} was derived and D_{0zdr} values were corrected by this relationship in the following analysis.

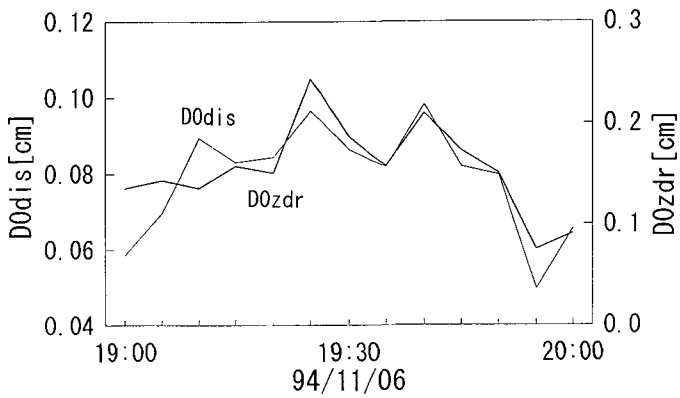

Fig. 8. Time series of the median volume drop diameter. D_{0dis} and D_{0zdr} which were estimated by disdrometer and polarimetric radar, respectively.

$$D_{0dis}=0.383\ D_{0zdr}+0.0195.$$

Figure 9 shows the vertical profile of horizontal reflectivity Z_h and median volume diameter D_0 at 21 : 30 JST on November 6. D_0 values were estimated from Z_{DR} above the radar-2 site selected from the observed RHI data and then corrected by the method mentioned above. Rainfall rate measured by the disdrometer was 7.53 mm/h. D_0 is displayed for the range of height below the bright band where hydrometeors were expected to be raindrops.

On the other hand, the bright band was not clear and Z_h increased with lowering height and reached a maximum value (20.4 dBZ) at a height of 1.0 km at 21 : 30 JST as shown in Fig. 9. Although the Z_{DR} value at 2.0 km was the same as at 19 : 35 JST, the maximum Z_{DR} value (3.2 dB) was observed at a height of 0.75 km in the lower layer. Since Z_h and D_0 show a greater increasing tendency with lowering height and larger values than at 19 : 35 JST below the bright band, it is suggested that growth of raindrops and broadening of drop size distribution by convection occurred in the lower layer.

5. Discussion

5.1 Estimation error in VPR method

Although the prefrontal rain band analyzed in the present paper is stratiform rain, we cannot assume that the vertical air speed is 0. In the case of vertical air velocity assumed to be 0, the calculated D_0 was about 2 times larger

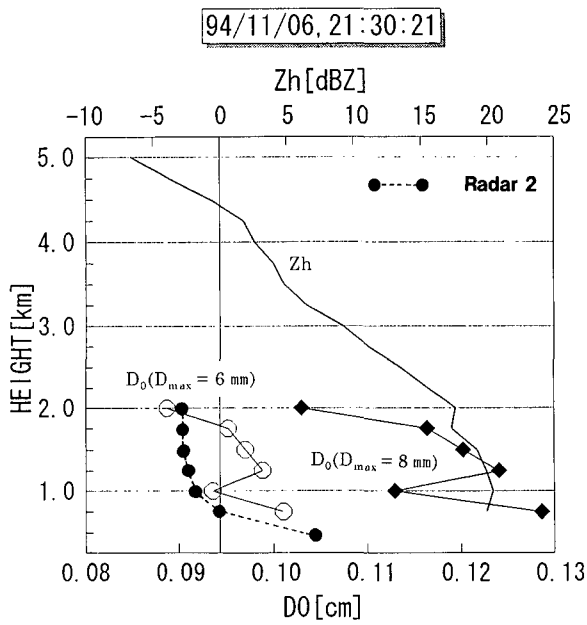

Fig. 9. Vertical profiles of horizontal reflectivity Z_h and median volume drop diameter D_0 estimated from Z_{DR} above the radar-2 site selected from the RHI data observed at 21 : 30 JST on November 6, 1994.

than disdrometer measured D_0 (not shown here). An updraft existed above the bright band during the majority of the period when the band was passing over the radar site.

Even when we considered vertical air speed, there was some discrepancy between D_{0_dis} derived by vertically pointing Doppler radar and D_{0_rad} measured by disdrometer for Nov. 11. D_{0_rad} was underestimated especially when the precipitation intensity was large. This is due to the estimation error related to vertical air velocity. The accuracy of the estimation of HSD by VPR method is dependent on the accuracy of Eq.(4). The estimation error in D_0 and N_0 caused by the error in $\overline{W}_t$ can be calculated by

$$\frac{dD_0}{D_0} = \frac{1}{b}\frac{d\overline{W}_t}{\overline{W}_t}$$

$$\frac{dN_0}{N_0} = -\frac{7}{b}\frac{d\overline{W}_t}{\overline{W}_t}.$$

The estimation errors for D_0 and N_0 are shown in Fig. 10 and Fig. 11 respectively. The accuracy of Eq.(4) for rain is 1 m/s (Joss and Waldvogel,

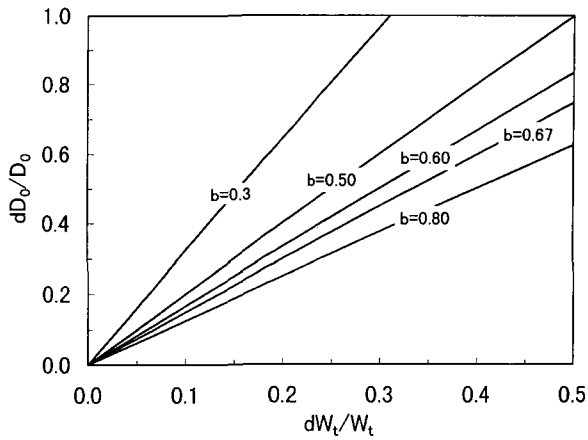

Fig. 10. Estimation error of D_0 for vertically pointing Doppler radar method. The parameter b is the power index of the equation of average terminal velocity, Eq. (2). $b=0.5, 0.6, 0.67$, and 0.8 are for rain and $b=0.3$ for snow.

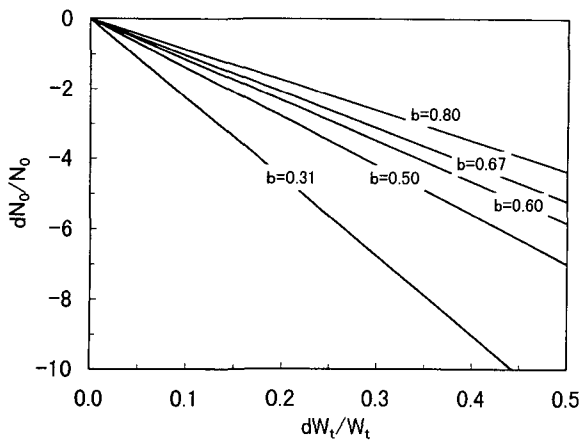

Fig. 11. As in Fig. 13 but with N_0.

1970) which corresponds to the relative error 20% for the particles falling with the terminal velocity of 5 m/s. This will cause about 20%-40% error in calculating D_0 depending on the value of the parameter b in Eq.(2). In the present study ($b=0.67$), the error is about 30%. However, in the case of snow ($b=0.3$), the same relative error in the terminal velocity causes about 60% error in calculating D_0. The estimation error in N_0 is large compared to the estimation

error in D_0. The relative error of 20% for terminal velocity will cause errors in N_0 of about 200% and 460% for rain and snow, respectively. More general considerations for estimation error by VPR method are discussed by Maki *et al.* (1998).

When terminal velocity is small, i.e., the rain rate is small or in the case of snow, the terminal velocity should be estimated more precisely.

5.2 Potential for POL method in studies on microphysics.

One of the difficulties with the POL method for estimating HSD parameters is due to the difficulty in the correction of attenuation effect for short wavelength radar systems such as a X-band radar. Seliga and Bringi (1976) showed that Z_{DR} should be measured with the accuracy of 0.2 dB for a reliable estimation of HSD. When the rain rate is great, it may be difficult to measure Z_{DR} within the accuracy of 0.2 dB because, the attenuation can not be neglected. However, a correction procedure for attenuation for X-band polarimetric radar is yet to be established.

Polarimetric radar has been recognized to be very useful in the discrimination between ice and liquid hydrometeors. Doviak and Zrnic (1993) summarized values of polarimetric parameters for various hydrometeor types from modeling, measurements, and experience of various researchers. Z_{DR} is a useful parameter in discriminating between rain and snow: Z_{DR} for rain (excepting drizzle) is from 0.5 to 4 while Z_{DR} for snow (dry and with low density) is close to zero (Aydin *et al.*, 1986). Although there are still difficult problems to overcome with X-band polarimetric radar, it is one of a number of useful and flexible tools to study the microphysics of precipitation and various related applications.

The potential for X-band polarimetric radar can be demonstrated by considering the structure of the observed prefrontal rain band. Two processes of the change in raindrop size distribution were found in the lower layer of stratiform precipitation clouds from the comparison of the vertical profiles of Z_h and D_0. One was the narrowing of drop size distribution when the bright band was clear. The bright band having maximum Z_h of 11.6 dBZ appeared at a height of 2.25 km and Z_{DR} had a maximum value (2.5 dB) at 2.0 km at 19 : 35 JST as shown in Fig. 12. The profile for Z_h shows little variation below the bright band and D_0 decreased from 0.103 to 0.080 cm with lowering height. It is suggested that raindrops partially evaporated and that raindrop size distribution became narrower. The other process was the broadening of drop size distribution accompanied with the growth of raindrops by convection when the bright band was not clear. As a result, rainfall rate on the ground was high in this

case compared to the former case.

5.3 *Notes on the position of sampling volume and averaging volume for VPR method and POL method*

As the structure of precipitation systems is not homogenous, it is important that we recognize that the position of the sampling volume and the averaging volume for VPR method is different from that for POL method. Even when we synthesize operations of vertically pointing Doppler and polarimetric radar systems as shown in Fig. 1, the estimated results by each method are sometimes different from each other. Estimation of D_0 for the C3 echo is a good example. The position of vertical profile of D_0 estimated by the POL method was at the edge of the C3 echo as shown by line a-a' in Fig. 4. The change in D_0 along the beam direction of the RHI scan of polarimetric radar may be large at the edge of the echo. On the other hand, the position of the time-height cross section by vertically pointing Doppler radar was at the inner side of the C3 echo as shown by line b-b' in Fig. 4. Comparison of these estimations shows different results. The vertical profile of D_0 estimated by the POL method showed a decrease in D_0 with decreasing height while D_0 estimated by the VPR method had the opposite

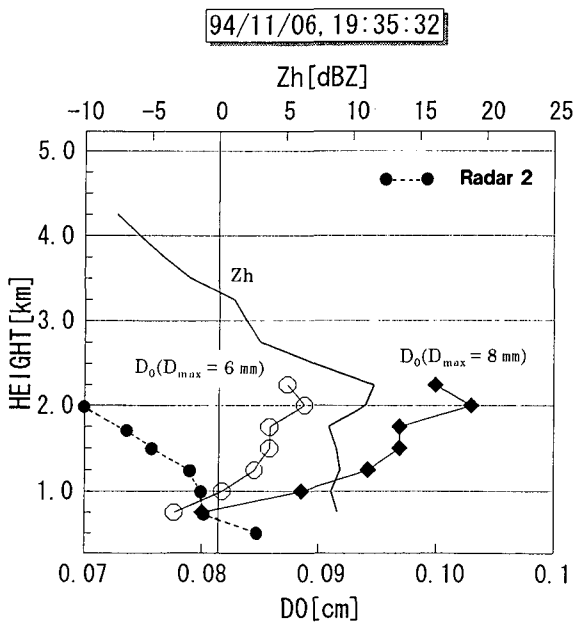

Fig. 12. As in Fig. 9 but with 19 : 30 JST.

tendency as shown in Fig. 12. This means estimations by the POL method represent a character at the edge of rainfalls; D_0 may decrease by evaporation of raindrops at the edge of the C3 echo. Considering that radar sampling volume is smaller for vertically pointing Doppler radar than for polarimetric radar, its estimation might not be affected by a character at the edge of an area of precipitation and may show the growth of raindrops inside the precipitation echo.

6. Concluding remarks

It was confirmed that estimation techniques for median volume diameter D_0 and vertical air speed by VPR method worked well in stratiform precipitation. Estimation errors for D_0 are about 30% and 60% for rain and snow respectively if there is estimation error of 20% in the averaged terminal hydrometeor velocity. However, the estimation errors of N_0 are about 200% for rain and 460% for snow. This is an essential to the VPR method as the estimation error of N_0 is more sensitive to estimation error of averaged terminal hydrometeor velocity.

The estimation of D_0 by the POL method was good only qualitatively in the present study. A correction algorithm for attenuation effects on X-band polarimetric radar is necessary for quantitative measurements in addition to development of a classification scheme which discriminates different types of hydrometeor such as rain, snow, graupel, hail and their mixture.

Acknowledgements

The authors would like to express their thanks to the Waterworks Bureau of the Sapporo City and Hotel Tenboukaku for giving every convenience for radar observations, and Mr. Kanemura of the Sapporo Information Network Inc. for the use of surface meteorological data.

References

Aydin, K., T.A. Seliga, and V. Balaij, 1986. Remote sensing of hail with a dual linear polarization radar. J. Climate Appl. Meteor., **25**, 1475-1484.

Atlas, D., R.C. Srivastava and R.S. Sekhon, 1973. Doppler radar characteristics of precipitation at vertical incidence. Rev. Geophys. Space Phys., **11**, 1-35.

Atlas, D. and C.W. Ulbrich, 1977. Path- and area-integrated rainfall measurement by microwave attenuation in the 1-3 cm band. J. Appl. Meteor., **16**, 1322-1331.

Caton, P.G.F., 1966. Raindrop size distribution in the free atmosphere. Quart. J. Roy. Meteor. Soc., **92**., 15-30.

Doviak, R.J., and D.S. Zrnic, 1993. Doppler radar and weather observations. Academic Press. 562pp.

Foote , G.B., and P.S. du Toit, 1969. Terminal velocities of raindrops aloft. J. Appl. Meteor., **8**, 249-253.

Gunn, K.L.S., and R.S. Marshall, 1958. The distribution of size of aggregate snowflakes. J. Meteor. **15**, 452-466.

Hauser, D., and P. Amayenc, 1981. A new method for deducing hydrometeor-size distribution and vertical air motions from Doppler radar measurements at vertical incidence. J. Appl. Meteor., **20**, 547-555.

Joss J., and A. Waldvogel, 1970. Raindrop size distributions and Doppler velocities. Preprint, 14th Radar Meteor. Conf., Boston: Amer. Meteor. Soc. 153-156.

Maki, M., T. Yagi and S. Nakai, 1989. The Doppler radar of NRCDP and observations of meso-scale weather systems (in Japanese with English abstract). Rep. Natl. Res. Cent. Disast. Prev., No. 44, 61-79.

Maki, M., Y. Sasaki and K. Iwanami, 1998. Accuracy of precipitation parameters estimated by vertically pointing Doppler radar observations (in Japanese with English abstract). Rep. Natl. Res. Inst. Earth Sci. Disast. Prev., No. 58 (in printing).

Rogers, R.R., 1964. An extension of the Z-R relation for Doppler radar. Proc. World Conf. Radar Meteor., 158-161.

Rogers, R.R, and R.J. Pilie, 1962. Radar measurements of drop-size distribution. J. Atmos. Sci., **19**, 503-508.

Sekhon, R.S., and R.C. Srivastava, 1971. Doppler radar observations of drop-size distribution in a thunderstorm. J. Atmos. Sci., **28**, 983-994.

Seliga, T.A. and V.N. Bringi, 1976. Potential use of radar differential reflectivity measurements at orthogonal polarizations for measuring precipitation. J. Appl. Meteor., **15**, 69-76.

Seliga, T.A., V.N. Bringi and H.H. Al-Khatib, 1981. A preliminary study of comparative measurements of rainfall rate using the differential reflectivity radar technique and a raingage network. J. Appl. Meteor., **20**, 1362-1368.